

Exploring the electronic, optical and charge transfer properties of acene-based organic semiconductor materials

AHMAD IRFAN^{1,*}, ABDULLAH G AL-SEHEMI¹, MOHAMMED A ASSIRI¹
and MUHAMMAD WASEEM MUMTAZ²

¹Department of Chemistry, Faculty of Science, King Khalid University, P.O. Box 9004, Abha 61413, Saudi Arabia

²Department of Chemistry, University of Gujrat, Gujrat, Punjab 50700, Pakistan

*Author for correspondence (irfaahmad@gmail.com)

MS received 9 October 2018; accepted 20 December 2018; published online 8 May 2019

Abstract. In order to tune the optoelectronic and charge transfer properties of 4,6-di(thiophen-2-yl)pyrimidine (**1**), some new compounds were designed, i.e., 4,6-bis(benzo[*b*]thiophen-2-yl)pyrimidine (**2**), 4,6-bis(naphtho[2,3-*b*]thiophen-2-yl)pyrimidine (**3**), 4,6-bis anthra[2,3-*b*]thiophen-2-yl)pyrimidine (**4**), 4,6-bis(tetraceno[2,3-*b*]thiophen-2-yl)pyrimidine (**5**) and 4,6-bis(pentaceno[2,3-*b*]thiophen-2-yl)pyrimidine (**6**). Compounds **2–6** were designed by assimilation of benzene, naphthalene, anthracene, tetracene and pentacene, respectively at both ends of compound **1**. Integration of oligocene end cores reduces the energy gap resulting in a red shift in the absorption and fluorescence emission spectra. The legible intra-molecular charge transfer is significant from electron-rich moieties to the electron-deficient core (pyrimidine). The elongation of π -conjugation led to escalate the electron affinity, lower the ionization potential and hole reorganization energy. The hole reorganization energies of compounds **3–6** exposed that these materials would be effective hole transport contenders to be used in diverse semiconductor devices.

Keywords. Organic thin film transistors (OTFTs); oligothiophenes; electron-deficient core; electro-optical properties; charge transfer.

1. Introduction

Recently, molecular electronics have gained increased interest especially in research and development of organic semiconductors which are being expected as new low-cost, flexible, lightweight, environment friendly, versatile and green approach in nature [1–8]. Organic semiconductors can be installed on several large area substrates at large scale production by decreasing manufacturing costs. The development of organic semiconductor materials (OSMs) is being under consideration for multifunctional purposes as organic light-emitting diodes, organic thin film transistors (OTFTs), photovoltaics, photodiodes etc. [9–21]. Due to variable quantity of OSMs, it is possible to modify at the molecular level. The design of specific materials with the desired energy gap, absorption and emission wavelengths is also conceivable. In OTFTs, the mobility is an important parameter which has already improved over the past ten years that is comparable to amorphous silicon. The organic π -conjugated materials especially acene-based molecules have significant research interest because of their prospective applications in OTFTs and OFETs. Now, the enduring determination is to enhance the carrier mobility of organic materials [21–23].

The first OTFT device was fabricated by polythiophene [24] and then in 1989 a small organic π -conjugated material,

i.e., sexithiophene was used [25]. Since two decades a lot of efforts has been emphasized on the thiophene and oligocene-based compounds to tune the optoelectronic and charge transport properties [26–31]. Additionally, oligothiophenes are also potential candidates for OTFT devices [32]. Hitherto, an electron transfer rate and efficiency have been improved by incorporating the electron-deficient moiety (pyrimidine) between the electron rich units [33,34].

Previously, functional properties of 4,6-di(thiophen-2-yl)pyrimidine (**1**) were tuned by strengthening the electron rich moieties, i.e., benzothiophene, naphthothiophene and anthrathiophene in 4,6-bis(benzo[*b*]thiophen-2-yl)pyrimidine (**2**), 4,6-bis(naphtho[2,3-*b*]thiophen-2-yl)pyrimidine (**3**) and 4,6-bis anthra[2,3-*b*]thiophen-2-yl)pyrimidine (**4**) [35]. In the present study, two more derivatives have been designed, i.e., 4,6-bis(tetraceno[2,3-*b*]thiophen-2-yl)pyrimidine (**5**) and 4,6-bis(pentaceno[2,3-*b*]thiophen-2-yl)pyrimidine (**6**) by incorporating the electron-deficient core (pyrimidine) in between tetracenothiophene and pentacenothiophene, respectively. Then various properties of interest were discussed and compared with the parent compound and its derivatives.

Among quantum chemical methods especially, density functional theory (DFT) is a good way to rationalize the experimental data of known materials and to predict the geometries, electronic, optical and charge transfer properties [36,37]. The effect of oligocene substituents was examined on the highest

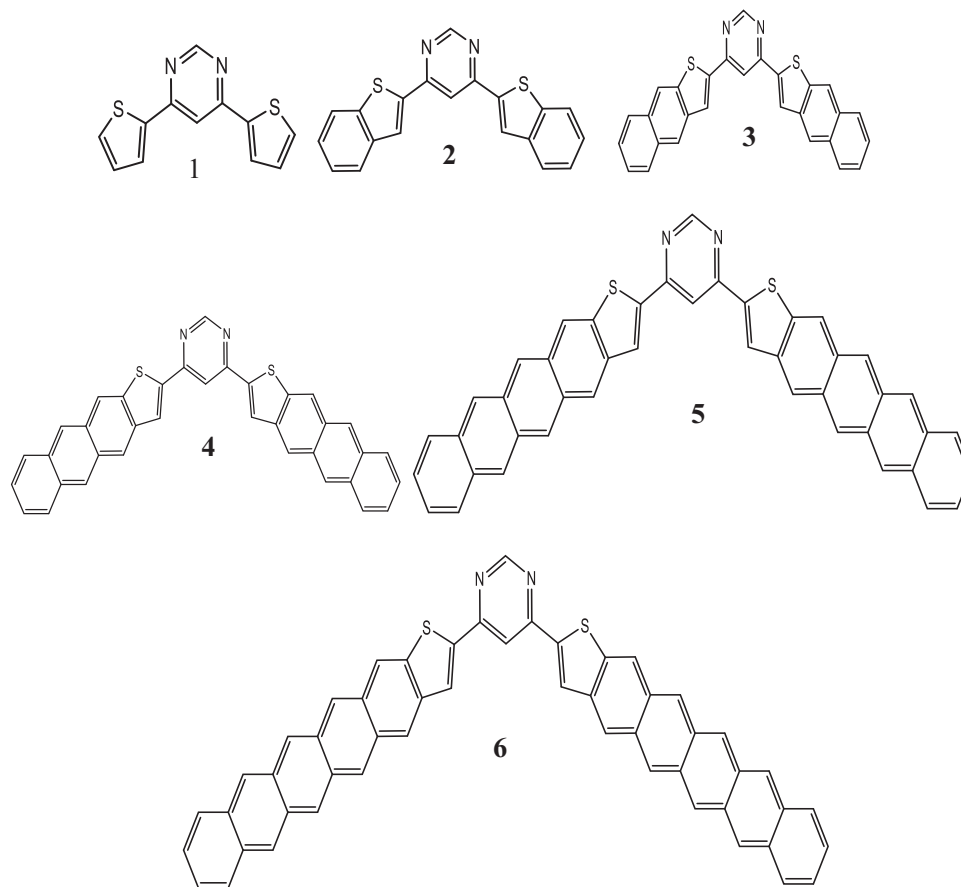


Figure 1. The structures of DTP and its derivatives investigated in the presented study.

occupied molecular orbital energies (E_{HOMO}), the lowest unoccupied molecular orbital energies (E_{LUMO}), the energy gap (E_g ; the difference between the E_{HOMO} and E_{LUMO}), absorption spectra (λ_{abs}), fluorescence emission spectra (λ_f), charge transport parameters, e.g., vertical/adiabatic ionization potentials ($\text{IP}_{\text{v/a}}$), vertical/adiabatic electron affinities ($\text{EA}_{\text{v/a}}$) and hole/electron reorganization energies ($\lambda_{\text{h/e}}$) and then compared with some reference compounds. The worthwhile information might shed some light towards the design of further multifunctional OTFT materials, see figure 1.

2. Methodology

Previously, it has been found that upon ionization B3LYP [38,39] of DFT [35,40–44] gave the best geometries as compared to other functionals [45]. Also, the experimental geometries were reproduced by DFT at the B3LYP [46] and 6-31G** basis set [47]. In the current study, the ground state (S_0) geometries of the neutral, anion and cation were optimized at the B3LYP/6-31G** level. The frequency calculations were performed at the same level to see the global minima. Any imaginary frequency was found revealing that the optimized geometries are the stable ones with the lowest

energy. The excited state (S_1) geometries were optimized at time-domain DFT (TDDFT) [48] at the TD-B3LYP/6-31G** level. The energies of the frontier molecular orbitals at S_1 were computed from the optimized geometries at the TD-B3LYP/6-31G** level. Moreover, the TDDFT was proven to be an efficient approach to reproduce the experimental λ_{abs} and λ_f [49]. The λ_{abs} and λ_f of the parent molecule (1) at the TD-B3LYP/6-31G** level were observed at 327 and 353 nm which are in good agreement with the experimental data, i.e., 329 and 378 nm respectively [50]. The λ_{abs} and λ_f were calculated by applying the same level [51]. According to the Marcus theory, the charge transfer rate can be defined as [52]:

$$W = V^2/h(\pi/\lambda k_B T)^{1/2} \exp(-\lambda/4k_B T), \quad (1)$$

where primary parameters are transfer integral (V) and reorganization energy (λ); the first term needs to be maximized while the second one to be small for significant transport. The λ can be distributed into two terms, i.e., $\lambda_{\text{rel}}^{(1)}$ and $\lambda_{\text{rel}}^{(2)}$. $\lambda_{\text{rel}}^{(1)}$ and $\lambda_{\text{rel}}^{(2)}$ are the energies of the geometry relaxation from the neutral to charged state and vice versa, respectively [53].

$$\lambda = \lambda_{\text{rel}}^{(1)} + \lambda_{\text{rel}}^{(2)} \quad (2)$$

In the present study, the λ was calculated as [54]:

$$\begin{aligned} \lambda &= \lambda_{\text{rel}}^{(1)} + \lambda_{\text{rel}}^{(2)} \\ &= [E^{(1)}(V^{+/-}) - E^{(0)}(V^{+/-})] \\ &\quad + [E^{(1)}(V) - E^{(0)}(V)]. \end{aligned} \quad (3)$$

Here, $E^{(0)}(V)$ and $E^{(0)}(V^{+/-})$ are the energies (S_0) of the neutral and charged states, $E^{(1)}(V)$ is the energy of the neutral at the optimized charged geometry and $E^{(1)}(V^{+/-})$ is the energy of the charged state at the optimized neutral geometry. The $IP_{a/v}$ and $EA_{a/v}$ were calculated at the B3LYP/6-31G** level. The calculations were executed by the Gaussian 16 package [55].

3. Results and discussion

3.1 Electronic properties

The calculated E_{HOMO} , E_{LUMO} and E_g at S_0 and S_1 compounds (**1–6**) are illustrated in figure 2. The computed E_{HOMO} and E_{LUMO} are: **1** (−6.19, −1.94), **2** (−5.95, −2.16), **3** (−5.46, −2.34), **4** (−5.08, −2.50), **5** (−4.79, −2.64) and **6** (−4.58, −2.78) eV, whereas the trend for E_g is **1** (4.25) > **2** (3.79) > **3** (3.12) > **4** (2.58) > **5** (2.15) > **6** (1.80) eV. It can be seen from figure 2 that by elongating the π -bridge usually E_{HOMO} increased while E_{LUMO} decreased. The work function (ϕ) of Al is 4.08 eV [56]. The electron/hole injection energies for **1** are around (2.14 eV = −1.94 − (−4.08))/(2.11 eV = −4.08 − (−6.19)). Here −4.08, −1.94 and −6.19 eV are for ϕ of Al, LUMO and HOMO of DTP. The ϕ of gold (Au) is 5.1 eV and electron/hole injection energies for **1** are (3.16 eV = −1.94 − (−5.10))/(1.09 eV = −5.10 − (−6.19)). Thus by depressing/rising the $E_{\text{LUMO}}/E_{\text{HOMO}}$ level it would be gentle to obtain better electron/hole injection strength. The extension of oligocenes declines the electron injection barrier from Al/Au as **2** (1.48/2.50), **3** (1.74/2.76), **4** (1.58/2.60), **5** (1.44/2.46) and **6** (1.30/2.32). The hole injection barrier decreases from **1** to **6** as the π -bridge expanded. The hole injection barrier from Al/Au **2–6** is 1.87/0.85, 1.38/0.36, 1.00, 0.71 and 0.50 eV, respectively. It is accounted from the $E_{\text{LUMO}}/E_{\text{HOMO}}$ levels that the injection barrier would be reduced for the electron/hole which is revealing that by elongating the bridge efficient contenders as the electron/hole transport would be expected.

Similarly, the trend for E_g at S_1 has been found as **1** (3.92) > **2** (3.46) > **3** (2.89) > **4** (2.38) > **5** (1.91) > **6** (1.64) eV. It was detected that the E_g decreased by elongating the π -bridge from benzene to pentacene, see figure 2. At S_0 and S_1 , the formation of the HOMO charge density has been delocalized on thiophene, benzothiophene, naphthothiophene, anthracenothiophene, tetracenothiophene and pentacenothiophene

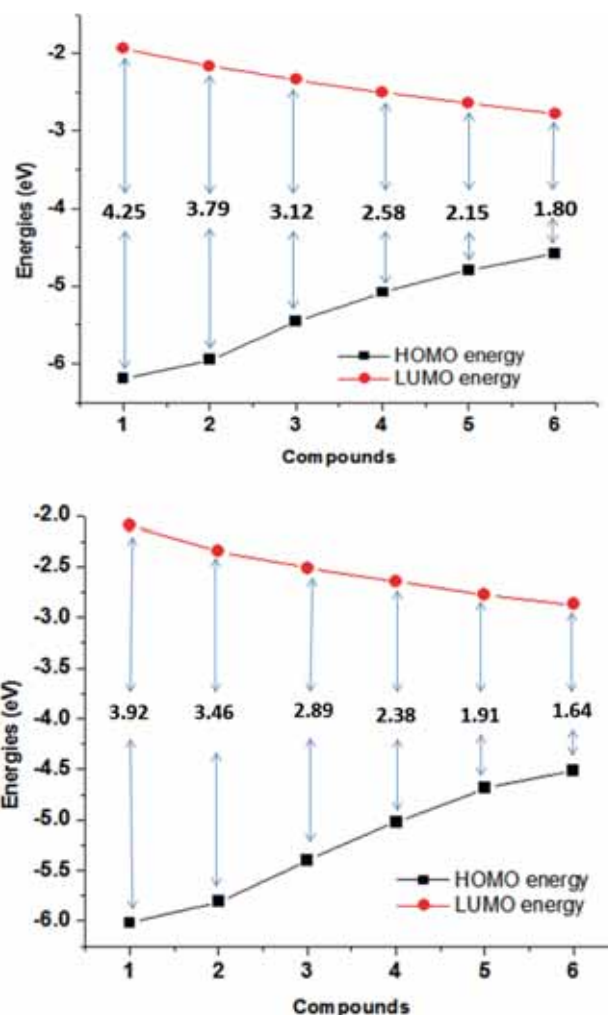


Figure 2. HOMO energies, LUMO energies and HOMO–LUMO energy gaps at ground states (top) and excited states (bottom).

in **1–6**, respectively. The LUMO is distributed on whole of the system. An intra-molecular charge transport has been observed from side moieties to the pyrimidine units (figure 3).

3.2 Photophysical properties

The computed λ_{abs} , λ_{f} , oscillator strengths (f) and dominant transitions at the TD-B3LYP/6-31G** level are illustrated in figure 4. The λ_{abs} and λ_{f} of the parent molecule at the TD-B3LYP/6-31G** level of theory have been observed at 327 and 353 nm which are in good agreement with the experimental data, i.e., 329 and 378 nm respectively [50]. The considerable transitions are H→L and L→H for the absorption and emission, respectively. Additionally, the second peak for the λ_{abs} and λ_{f} has been noticed at 280 and 292 nm with the transitions from H−1→L+1 and L→H−1, respectively. By introducing benzene at both the end cores the λ_{a} and λ_{f} are being red shifted, i.e., 40 and 44 nm in **2** with the main transitions from H→L and L→H, respectively compared to

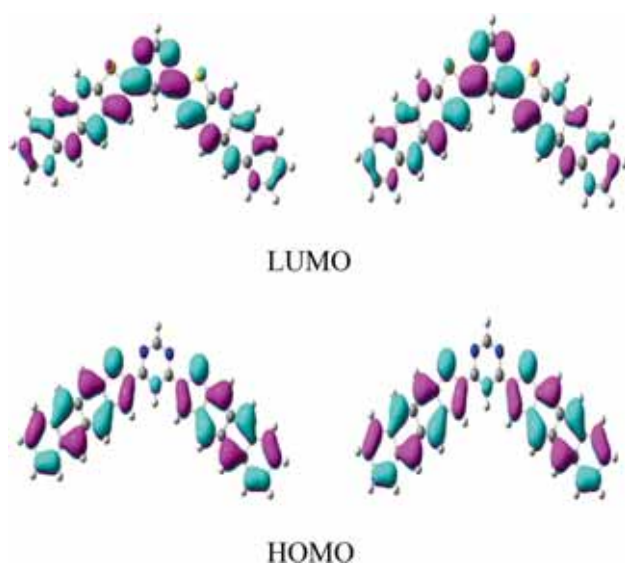


Figure 3. Distribution pattern of the HOMOs and LUMOs of the representative compound (**4**) at the ground state (left) and excited state (right).

the parent molecule (**1**). Naphthalene at both the ends lead the λ_a and λ_f towards the red shift, i.e., 123 and 134 nm in **3** with the transitions from H \rightarrow L and L \rightarrow H, respectively compared to **1**. Another peak has also been observed in **3** which is being 28 and 16 nm red shifted than the parent molecule with the transitions from H-2 \rightarrow L and L \rightarrow H-2, respectively.

The fusion of anthracene at both the ends also led the λ_a and λ_f towards the red shift, i.e., 220 and 241 nm in **4** with the transitions from H \rightarrow L and L \rightarrow H, respectively compared to **1**. The second peak has been detected that is being 43 and 31 nm red shifted compared to **1** with the transitions from H-2 \rightarrow L and L \rightarrow H-2, respectively. The addition of tetracene at the

both ends of the parent molecule resulted in the red shift in the λ_a and λ_f , i.e., 337 and 336 nm in **5** with the transitions from H \rightarrow L and L \rightarrow H-1, respectively compared to **1**. The second peak has been noticed that is being 93 and 79 nm red shifted compared to **1** with the transitions from H-2 \rightarrow L and L+3 \rightarrow H, respectively. The introduction of pentacene at the both ends of the parent molecule ensured a red shift in the λ_a and λ_f , i.e., 468 and 467 nm in **6** with the transitions from H \rightarrow L and L \rightarrow H-1, respectively compared to **1**. The second peak has been discerned which is being 222 and 227 nm red shifted compared to **1** with the transitions from H \rightarrow L+2 and L+2 \rightarrow H, respectively.

3.3 Charge transport properties

To understand the charge transport abilities of the organic compounds IP and EA play a significant role. Usually, higher EA and lower IP would lead to the higher electron and hole transport, respectively. In the present study, we have computed the $IP_{a/v}$ and $EA_{a/v}$ of all the compounds **1-6** at the B3LYP/6-31G** level and shown in figure 5. The IP_a (IP_v) values of **2-6** are 0.44 (0.48), 1.08 (1.14), 1.58 (1.65), 1.95 (2.02) and 2.23 (2.31) eV smaller than those of the parent compound, respectively. The EA_a (EA_v) values of **2-6** are 0.43 (0.43), 0.75 (0.77), 1.02 (1.06), 1.27 (1.33) and 1.49 (1.56) eV larger than those of the parent molecule, respectively. Here, it can be found that by elongating the π -conjugation at both the ends of **1**, IP is being small while EA larger than the parent molecule. This observation revealed that it would lower the charge injection barrier for the hole and electron in new designed derivatives **2-6** resulting in improving the hole and electron charge injection ability than the parent molecule.

There is another imperative parameter which help in comprehending the capability of a compound to transport the charge in solid, i.e., reorganization energy (λ) [54,57]. Here,

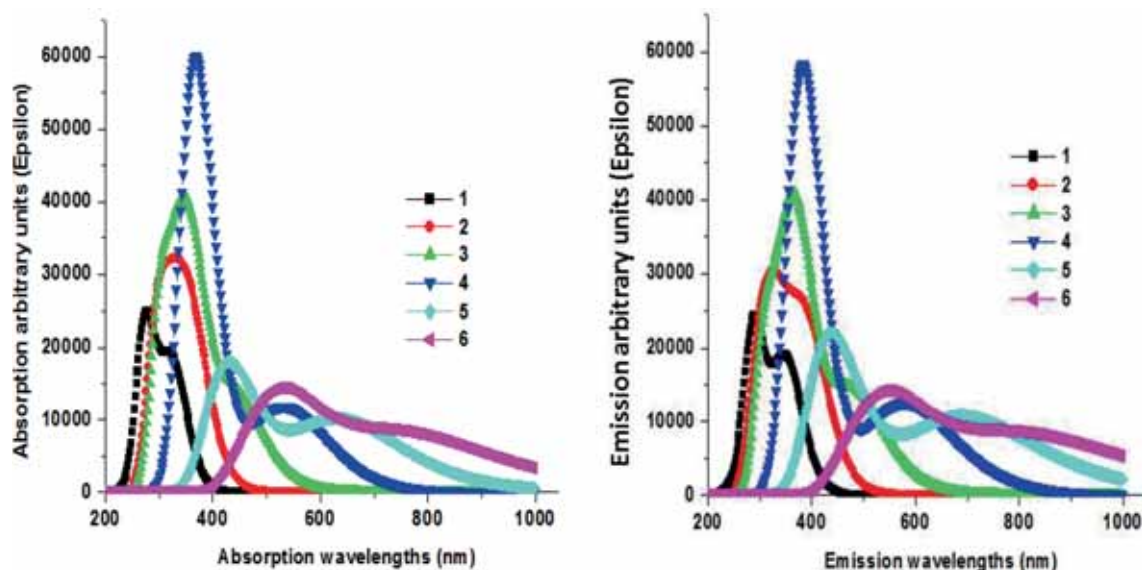


Figure 4. The absorption (left) and fluorescence emission spectra (right) of DTP and its derivatives.

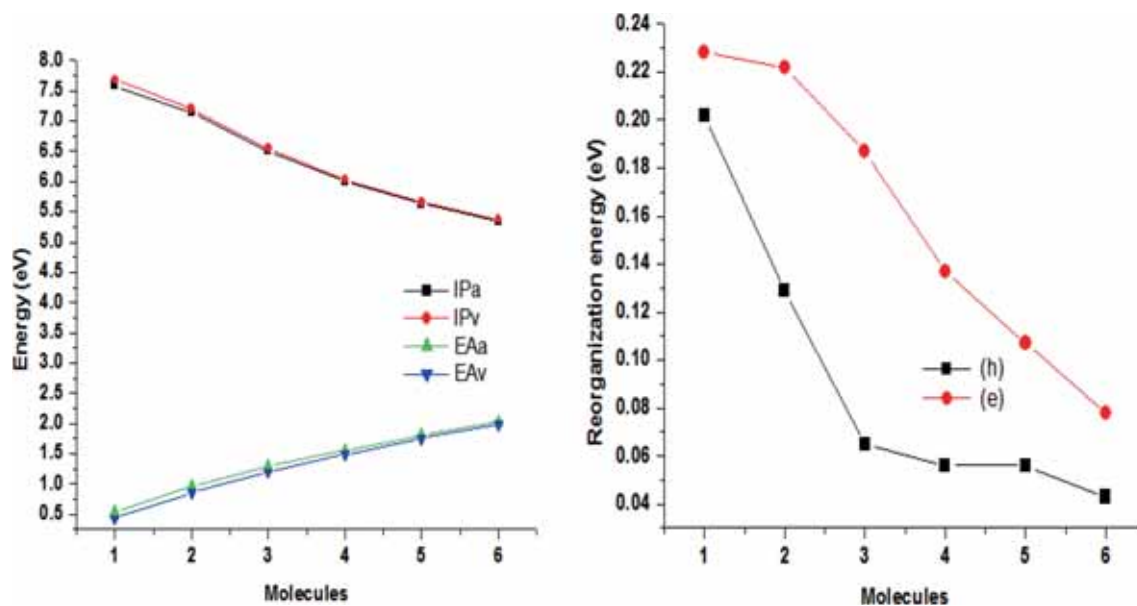


Figure 5. Graphical representation of IP_v , IP_a , EA_v and EA_a (left) while $\lambda(h)$ and $\lambda(e)$ (right) calculated at the B3LYP/6-31G** level of theory.

the hole and electron reorganization energies ($\lambda(h)$ and $\lambda(e)$) have been calculated at the B3LYP/6-31G** level and are shown in figure 5. The fusion of benzene, naphthalene, anthracene, tetracene and pentacene at both the ends of the parent molecule significantly lower the $\lambda(h)$ and $\lambda(e)$. The $\lambda(h)$ and $\lambda(e)$ of all the newly designed derivatives have been compared with distinguished referenced compounds to understand the charge transport performance. The computed values of $\lambda(h)$ of 2–6 are 0.073, 0.137, 0.146, 0.146 and 0.159 eV smaller than those of the parent molecule, respectively revealing that by elongating the π -bridge would lead to enhance the hole transport properties. However, the $\lambda(e)$ values of 2–6 are 0.006, 0.041, 0.091, 0.121 and 0.150 eV smaller than those of the parent molecule, respectively illuminating that by extending the π -bridge would lead to boost up the electron transport properties. Additionally, the computed $\lambda(h)$ values of 1–6 are smaller than the $\lambda(e)$ enlightening that all the studied compounds might be better hole transport materials than the electron ones.

The $\lambda(h)$ of benzo[1,2-*b*:5,4-*b'*]dithiophene, naphtho[2,3-*b*:6,7-*b'*]dithiophene, naphtho[2,3-*b*:7,6-*b'*]dithiophene, anthra[2,3-*b*:7,8-*b'*]dithiophene, anthra[2,3-*b*:8,7-*b'*]dithiophene, thieno[2,3-*f*:5,4-*f'*]bis[1]benzothiophene and thieno[3,2-*f*:4,5-*f'*]bis[1]benzothiophene are 0.108, 0.106, 0.100, 0.096, 0.094, 0.118 and 0.146 eV [58]. The $\lambda(h)$ of 3 is 43, 41, 35, 31, 29, 53, 81; 4 and 5 are 52, 50, 44, 40, 38, 62 and 90; 6 is 65, 63, 57, 53, 51, 75 and 103 meV smaller than the $\lambda(h)$ of benzo[1,2-*b*:5,4-*b'*]dithiophene, naphtho[2,3-*b*:6,7-*b'*]dithiophene, naphtho[2,3-*b*:7,6-*b'*]dithiophene, anthra[2,3-*b*:7,8-*b'*]dithiophene, anthra[2,3-*b*:8,7-*b'*]dithiophene, thieno[2,3-*f*:5,4-*f'*]bis[1]benzothiophene and thieno[3,2-*f*:4,5-*f'*]bis[1]benzothiophene, respectively [58]. Pentacene

is an efficient hole transport material which is being used in OTFT devices. Gruhn *et al* [59] concluded that the reorganization energy is the important parameter which allows pentacene to prove the predominantly greater mobility. Previously, the $\lambda(h)$ of pentacene was calculated to be 0.098 eV [60]. It can be seen from figure 5 that the $\lambda(h)$ values of 3–6 are 33, 42, 42 and 55 meV smaller than those of the referenced compound, i.e., pentacene, respectively showing that these new designed materials might be good/commensurate hole transfer contenders to pentacene. Furthermore, the computed $\lambda(e)$ of a renowned and frequently used electron transfer material meridional-tris(8-hydroxyquinolino)aluminium (*mer*-Alq3) is 0.276 eV [61]. We found that the $\lambda(e)$ values of 1–6 are 48, 54, 89, 139, 169 and 198 meV smaller than *mer*-Alq3 specifying that electron mobility of these studied compounds 1–6 might be better/corresponding to *mer*-Alq3.

4. Conclusions

The incorporation of elongated π -bridge increased the HOMO energy while decreased the LUMO energy values. The electron and hole injection barrier decrease as $2 > 3 > 4 > 5 > 6$. The energy gap is also decreased by elongating the π -bridge from benzene to pentacene. An intra-molecular charge transport was observed from the oligocene to pyrimidine moiety. By introducing the oligocene units at both the ends of DTP leads to a red shift in the absorption and fluorescence. The fusion of oligocene at the end cores leads to reduction in the IP and an increase in the EA values resulting in the development of hole and electron charge injection ability as compared to the parent compound. The incorporation of benzene, naphthalene, anthracene, tetracene and pentacene at both the ends

of DTP considerably lower the hole and electron reorganization energies as well. Based on the reorganization energy, it seems that studied compounds might be better hole transport materials. The hole reorganization energies of compounds **3–6** are 33, 42, 42 and 55 meV smaller than those of pentacene, respectively displaying that prior derivatives might be good/comparable hole transport contenders to pentacene. The electron reorganization energy values of **1–6** are 48, 54, 89, 139, 169 and 198 meV smaller than those of *mer*-Alq₃ illuminating that electron mobility of compounds **1–6** might be better/comparable to *mer*-Alq₃.

Acknowledgements

The authors extend their appreciation to the Deanship of Scientific Research at King Khalid University for funding this work through research groups program under grant number R.G.P.1/18/40.

References

- [1] Reimers J R, Picconatto C A, Ellenbogen J C and Shashidhar R 2003 *Molecular electronics IH* (New York Academy of Science) **1006**
- [2] Wazzan N and Irfan A 2018 *Org. Electron.* **63** 328
- [3] Wazzan N, El-Shishtawy R M and Irfan A 2017 *Theor. Chem. Acc.* **137** 9
- [4] Habib M, Ghosh N N, Sarkar R, Pramanik A, Sarkar P and Pal S 2018 *Chem. Phys. Lett.* **709** 21
- [5] Pramanik A, Sarkar S, Pal S and Sarkar P 2015 *Phys. Lett. A* **379** 1036
- [6] Bouit P-A, Infantes L, Calbo J, Viruela R, Ortí E, Delgado J L *et al* 2013 *Org. Lett.* **15** 4166
- [7] Habib M, Saha S, Sarkar R, Pramanik A, Sarkar P and Pal S 2018 *Comput. Theor. Chem.* **1136–1137** 10
- [8] Roy P, Biswas S, Pramanik A and Sarkar P 2018 *Chem. Phys. Lett.* **708** 87
- [9] Irfan A, Muhammad S, Al-Sehemi A G, Al-Assiri M S, Kalam A and Chaudhry A R 2015 *J. Theor. Comput. Chem.* **14** 1550027
- [10] Irfan A, Al-Sehemi A G and Al-Assiri M S 2014 *Comput. Theor. Chem.* **1031** 76
- [11] Şengez B, Doğruyol Z, San S E, Kösemen A, Yılmaz F, Okutan M *et al* 2013 *Microelectron. Eng.* **103** 111
- [12] Szlachcic P, Danel K S, Gryl M, Stadnicka K, Usatenko Z, Nosidlak N *et al* 2015 *Dyes Pigm.* **114** 184
- [13] Jungsuttiwong S, Tarsang R, Surakhot Y, Khunchalee J, Sudyoadsuk T, Promarak V *et al* 2012 *Org. Electron.* **13** 1836
- [14] Marks T J and Hersam M C 2015 *Nature* **520** 631
- [15] Arunkumar A, Prakasam M and Anbarasan P M 2017 *Bull. Mater. Sci.* **40** 1389
- [16] Ghosh N N, Habib M, Pramanik A, Sarkar P and Pal S 2018 *Bull. Mater. Sci.* **41** 56
- [17] Kumar M S, Charanadhar N, Srikanth V V S S, Rao K B S and Raj B 2018 *Bull. Mater. Sci.* **41** 62
- [18] Wang D, Huang S, Wang C, Yue Y and Zhang Q 2019 *Org. Electron.* **64** 216
- [19] Li M, Kou L, Diao L, Zhang Q, Li Z, Wu Q *et al* 2015 *J. Phys. Chem. A* **119** 3299
- [20] Biswas S, Pramanik A, Pal S and Sarkar P 2017 *J. Phys. Chem. C* **121** 2574
- [21] Tarsang R, Promarak V, Sudyoadsuk T, Namuangruk S, Kungwan N, Khongpracha P *et al* 2015 *RSC Adv.* **5** 38130
- [22] Park G E, Shin J, Lee D H, Lee T W, Shim H, Cho M J *et al* 2014 *Macromolecules* **47** 3747
- [23] Back J Y, Kim Y, An T K, Kang M S, Kwon S-K, Park C E *et al* 2015 *Dyes Pigm.* **112** 220
- [24] Tsumura A, Koezuka H and Ando T 1986 *Appl. Phys. Lett.* **49** 1210
- [25] Horowitz G, Fichou D, Peng X, Xu Z and Garnier F 1989 *Solid State Commun.* **72** 381
- [26] Thompson B C and Fréchet J M J 2008 *Angew. Chem. Int. Edit.* **47** 58
- [27] Tang M L, Okamoto T and Bao Z 2006 *J. Am. Chem. Soc.* **128** 16002
- [28] Minemawari H, Yamada T, Matsui H, Tsutsumi J Y, Haas S, Chiba R *et al* 2011 *Nature* **475** 364
- [29] Pethig R and Morgan K 1967 *Nature* **214** 266
- [30] Jung K H, Bae S Y, Kim K H, Cho M J, Lee K, Kim Z H *et al* 2009 *Chem. Commun.* <https://doi.org/10.1039/b911780f5290>
- [31] Chung D S, Park J W, Park J-H, Moon D, Kim G H, Lee H-S *et al* 2010 *J. Mater. Chem.* **20** 524
- [32] Horowitz G and Hajlaoui M E 2000 *Adv. Mater.* **12** 1046
- [33] Guo M, He R, Dai Y, Shen W, Li M, Zhu C *et al* 2012 *J. Phys. Chem. C* **116** 9166
- [34] Irfan A, Al-Sehemi A G and Muhammad S 2014 *Synth. Met.* **190** 27
- [35] Irfan A, Chaudhry A R, Al-Sehemi A G, Sultan Al-Asiri M, Muhammad S and Kalam A 2016 *J. Saudi Chem. Soc.* **20** 336
- [36] Irfan A, Chaudhry A R, Muhammad S and Al-Sehemi A G 2017 *J. Mol. Graph. Modell.* **75** 209
- [37] Irfan A, Cui R, Zhang J and Nadeem M 2010 *Aust. J. Chem.* **63** 1283
- [38] Kohn W, Becke A D and Parr R G 1996 *J. Phys. Chem.* **100** 12974
- [39] Becke A D 1993 *J. Chem. Phys.* **98** 5648
- [40] Irfan A, Kalam A, Chaudhry A R, Al-Sehemi A G and Muhammad S 2017 *Optik* **132** 101
- [41] Irfan A, Al-Sehemi A G, Chaudhry A R and Muhammad S 2017 *Optik* **138** 349
- [42] Irfan A and Mahmood A 2018 *J. Clust. Sci.* **29** 359
- [43] Irfan A, Assiri M and Al-Sehemi A G 2018 *Org. Electron.* **57** 211
- [44] Irfan A and Abbas G 2018 *Z. Naturforsch. A* **73** 337
- [45] Sánchez-Carrera R S, Coropceanu V, da Silva Filho D A, Friedlein R, Osikowicz W, Murdey R *et al* 2006 *J. Phys. Chem. B* **110** 18904
- [46] Lee C, Yang W and Parr R G 1988 *Phys. Rev. B* **37** 785
- [47] Petersson G A, Bennett A, Tensfeldt T G, Al-Laham M A, Shirley W A and Mantzaris J 1988 *J. Chem. Phys.* **89** 2193
- [48] Furche F and Ahlrichs R 2002 *J. Chem. Phys.* **117** 7433
- [49] Zhang C, Liang W, Chen H, Chen Y, Wei Z and Wu Y 2008 *J. Mol. Struct. (TheoChem)* **862** 98
- [50] Dufresne S, Hanan G S and Skene W G 2007 *J. Phys. Chem. B* **111** 11407
- [51] Chaudhry A R, Ahmed R, Irfan A, Shaari A and Al-Sehemi A G 2013 *Mater. Chem. Phys.* **138** 468

- [52] Marcus R A and Sutin N 1985 *Biochim. Biophys. Acta (BBA) - Rev. Bioenerg.* **811** 265
- [53] Tsiper E V, Soos Z G, Gao W and Kahn A 2002 *Chem. Phys. Lett.* **360** 47
- [54] Brédas J L, Calbert J P, da Silva Filho D A and Cornil J 2002 *Proc. Natl. Acad. Sci. USA* **99** 5804
- [55] Frisch M J, Trucks G W, Schlegel H B, Scuseria G E, Robb M A, Cheeseman J R *et al* 2016 *Gaussian*
- [56] http://www2.chemistry.msu.edu/faculty/harrison/cem483/work_functions.pdf
- [57] Marcus R A 1993 *Rev. Mod. Phys.* **65** 599
- [58] Irfan A, Chaudhry A R, Al-Sehemi A G, Sultan Al-Asiri M, Muhammad S and Kalam A 2014 *J. Saudi Chem. Soc.* <https://doi.org/10.1016/j.jscs.2014.09.009>
- [59] Gruhn N E, da Silva Filho D A, Bill T G, Malagoli M, Coropceanu V, Kahn A *et al* 2002 *J. Am. Chem. Soc.* **124** 7918
- [60] Bromley S T, Mas-Torrent M, Hadley P and Rovira C 2004 *J. Am. Chem. Soc.* **126** 6544
- [61] Irfan A, Cui R, Zhang J and Hao L 2009 *Chem. Phys.* **364** 39